

A new strategy to optimize complex absorbing potentials for the computation of resonance energies and widths

Jerryman A. Gyamfi* and Thomas-C. Jagau*

Department of Chemistry, KU Leuven, Celestijnenlaan 200F, B-3001 Leuven, Belgium

E-mail: jerrymanappiahene.gyamfi@kuleuven.be; thomas.jagau@kuleuven.be

Abstract

Complex absorbing potentials (CAPs) are artificial potentials added to electronic Hamiltonians to make the wave function of metastable electronic states square-integrable. This makes electronic-structure theory of resonances comparable to that of bound states, thus reducing the complexity of the problem. However, the most often used box and Voronoi CAPs depend on several parameters that have a substantial impact on the numerical results. Among these parameters are the CAP strength and a set of spatial parameters that define the onset of the CAP. It has been a common practice to minimize the perturbation of the resonance states due to the CAP by optimizing the strength parameter while fixing the onset parameters although the performance of this approach strongly depends on the chosen onset.

Here we introduce a more general approach that allows one to optimize not only the CAP strength but also the spatial parameters. We show that fixing the CAP strength and optimizing the spatial parameters is a reliable way for minimizing CAP perturbations. We illustrate the performance of this new approach by computing resonance energies and widths of the temporary anions of dinitrogen, ethylene, and formic acid.

This is done at the Hartree-Fock and equation-of-motion coupled-cluster singles and doubles levels of theory, using full and projected box and Voronoi CAPs.

1 Introduction

Owing to their role in diverse fields of science including biochemistry,^{1,2} astrophysics,³ and plasma chemistry⁴ research on temporary anions (TAs) has seen a significant increase over the last decades.^{5,6} TAs are metastable electronic states, also called resonances,⁷⁻⁹ with a lifetime in the range of femto- to milliseconds that are formed when a molecule with zero electron affinity captures an electron. Because resonances are embedded in the continuum of the electronic Hamiltonian, it is challenging to study TAs by means of conventional quantum chemistry methods that were designed for bound states.

Besides approaches based on scattering theory,^{10,11} complex-variable techniques offer a way to study TAs. Here, the objective is to make the diverging resonance wave functions square-integrable so that electronic-structure methods similar to those developed for bound states can be applied. Among complex-variable techniques are complex scaling,¹²⁻¹⁴ where the electronic coordinates in the Hamiltonian are scaled by a complex number, the method of complex basis functions,¹⁵⁻¹⁷ where one employs Gaussian basis functions with complex-scaled exponents, and complex absorbing potentials¹⁸⁻²¹ (CAPs), where an imaginary potential is added to the Hamiltonian. These methods all come with the advantage that explicit representation of the continuum is not necessary for the description of a resonance but they render the Hamiltonian non-Hermitian. In non-Hermitian quantum mechanics,⁷ the usual inner product is replaced by the so-called c-product²² and expectation values can, in general, be complex-valued.

Among the different complex-variable techniques, CAP methods are most widely used to study TAs. By creating an absorbing region where artificial damping takes place, the CAP makes the diverging wave function of a TA square-integrable so that it can be represented

in a basis set of Gaussian functions.²⁰ The electronic Hamiltonian H is modified according to

$$H_{\text{CAP}} = H - i\eta W , \quad (1)$$

where η is usually a real scalar and W a Hermitian operator. The associated Schrödinger equation

$$H_{\text{CAP}}|\Psi\rangle = (E_r - i\Gamma/2)|\Psi\rangle \quad (2)$$

has complex Siegert energies,²³ where E_r is the resonance energy and Γ is the resonance width, which is related to the lifetime τ as $\Gamma = 1/\tau$.

Different functional forms have been proposed for the CAP W .^{20,21,24-32} In this work, we shall be concerned with box CAPs²⁰ and smooth Voronoi CAPs,³² which are most widely used to study molecular TAs. For both types of CAP, W is a one-electron operator that is further specified by a set of parameters, which define the spatial boundary between two regions: the outer one where the CAP is active and the inner one where it is not. With a box CAP, the boundary is a cuboid box, which in Cartesian coordinates is defined by three parameters r_x^0, r_y^0, r_z^0 . Most often, the CAP is chosen to be quadratic in the electronic coordinates even though higher powers have been used as well.²⁰ The operator W is thus defined as

$$W = \sum_{\alpha=x,y,z} W_{\alpha} , \quad (3)$$

$$W_{\alpha} = \begin{cases} (|r_{\alpha} - o_{\alpha}| - r_{\alpha}^0)^2 & \text{if } |r_{\alpha} - o_{\alpha}| > r_{\alpha}^0 \\ 0 & \text{else} \end{cases} \quad (4)$$

with r_{α} as the electronic coordinate along axis α and the vector (o_x, o_y, o_z) as the origin of the CAP.

With the smooth Voronoi CAP, the boundary is constructed from each nucleus' Voronoi cell with the sharp edges between the cells smoothed out.³² Here, the operator W depends

on a single spatial parameter r^0 and is defined as³²

$$W(\mathbf{r}) = \begin{cases} (r_{\text{av}}(\mathbf{r}) - r^0)^2 & \text{if } r_{\text{av}} > r^0 \\ 0 & \text{else} \end{cases} \quad (5)$$

where the weighted average of electron-nuclei distances r_{av} is given as

$$r_{\text{av}}(\mathbf{r}) = \sqrt{\sum_I w_I(\mathbf{r}) r_I^2(\mathbf{r}) / \sum_I w_I(\mathbf{r})} \quad (6)$$

and the weights w_I are given as $w_I = (r_I^2 - r_{\text{nearest}}^2 + 1)^{-2}$ with $r_{\text{nearest}}(\mathbf{r}) = \min_I(|\mathbf{r} - \mathbf{R}_I|)$. Smooth Voronoi CAPs are especially recommended for molecules whose structure is incompatible with a cuboid box.

The introduction of the CAP can lead to a strong perturbation of the physical Hamiltonian H from Eq. (1) and, consequently, a wrong description of the resonance. For example, in our recent work on molecular dynamics of TAs,³³ we showed how using unsuitable CAP parameters may lead to an incorrect description of the time evolution. To obviate such problems, it is imperative to make sure that the CAP is just a small perturbation to H . How to achieve this has been an important subject since the advent of the CAP method.^{20,27,29,30,34,35}

In molecular electronic-structure calculations, the prevailing way of minimizing the perturbation is through optimizing only the strength parameter η , which is done according to²⁰

$$\min |\eta dE(\eta)/d\eta| . \quad (7)$$

In contrast, there is no consensus on how to choose the onset parameters \mathbf{r}^0 . For box CAP calculations on TAs, it has been suggested to use the second moment of the electron density of the parent neutral molecule in order to avoid optimization of \mathbf{r}^0 on a case-by-case basis.³⁵⁻³⁷ This approach has proved useful in the study of electronic resonances but it is undeniable that in some cases the resonance is strongly perturbed by the CAP. Even worse, in other

cases one fails to determine an optimal value of η by means of Eq. (7) or one is unable to distinguish resonances and pseudo-continuum states.

In this work, we explore an alternative to Eq. (7): We use a more general criterion that has the expectation value of the CAP, $\langle -i\eta W \rangle$, at its center. In this way, it becomes possible to optimize any CAP parameter, not just η . Specifically, we show that optimizing the onset \mathbf{r}^0 while keeping η fixed is an effective strategy for determining energies and widths of TAs.

The remainder of the article is organized as follows: In Sec. 2 we give a short review on the derivation of Eq. (7) and introduce our new criterion. Sec. 3 summarizes the details of some illustrative calculations on the TAs of dinitrogen, ethylene, and formic acid, the results of which are presented in Sec. 4. This is followed by final remarks in Sec. 5.

2 Theory

2.1 Optimization of the CAP strength using the established procedure

We start by briefly revisiting the origin of Eq. (7). Our arguments below are similar to the original arguments put forward in Ref. 20. We consider Eqs. (1) and (2) assuming that we have fixed the spatial parameters \mathbf{r}^0 and want to minimize the CAP reflections by optimizing the value of η . We take the unknown true Siegert energy E_0 as reference, while $E(\eta)$ represents the complex-valued energy computed at a given η .

We introduce an error function $\epsilon(\eta)$ as

$$\epsilon(\eta) := E(\eta) - E_0, \quad (8)$$

which, naturally, is also unknown to us like E_0 . It has been shown for a wide variety of CAPs including those from Eqs. (3) and (5) that, in a complete basis set, $E(\eta)$ will approach E_0

for vanishing CAP strength,²⁰ i.e., $\lim_{\eta \rightarrow 0} \epsilon(\eta) = 0$. For a finite basis set, we may expand $\epsilon(\eta)$ into a Maclaurin series because we expect η_{opt} to be in the neighborhood of $\eta = 0$. This yields

$$\epsilon(\eta) = \epsilon(0) + \sum_{n=1} \frac{\eta^n}{n!} \left. \frac{d^n \epsilon(\eta')}{d\eta'^n} \right|_{\eta'=0} . \quad (9)$$

The constant $\epsilon(0) = E(\eta = 0) - E_0$ is also unknown. In first order of η , the absolute error $|\epsilon|$ has the expression

$$|\epsilon(\eta)| = |E(\eta) - E_0| = \left| \epsilon(0) + \eta \left. \frac{d\epsilon(\eta')}{d\eta'} \right|_{\eta'=0} \right| \leq |\epsilon(0)| + \left| \eta \left. \frac{d\epsilon(\eta')}{d\eta'} \right|_{\eta'=0} \right| \quad (10)$$

where the triangle inequality is applied in the last step. Since $|\epsilon(0)|$ is unknown, we may minimize $|\epsilon(\eta)|$ by minimizing $\left| \eta \left. \frac{d\epsilon(\eta')}{d\eta'} \right|_{\eta'=0} \right| = \left| \eta \left. \frac{dE(\eta')}{d\eta'} \right|_{\eta'=0} \right|$.

If we further introduce the approximation

$$\eta \left. \frac{dE(\eta')}{d\eta'} \right|_{\eta'=0} \approx \eta \left. \frac{dE(\eta')}{d\eta'} \right|_{\eta'=\eta} \quad (11)$$

then we may consider $|\epsilon(\eta)|$ as minimized if we find an η such that Eq. (7) is satisfied. It also follows that a more accurate approximation to the true Siegert energy can be computed as

$$\tilde{E}(\eta) := E(\eta) - \eta \frac{dE(\eta)}{d\eta} \approx E_0 + \epsilon(0) \quad (12)$$

where $\tilde{E}(\eta)$ has been referred to as first-order deperturbed energy.^{20,35}

2.2 Optimization of arbitrary CAP parameters using a new error function

We propose that the CAP onset \mathbf{r}^0 be amenable to optimization when minimizing CAP reflections. To this end, we introduce an error function ξ which gauges how strong a perturbation the CAP contribution $-i\eta W$ is with respect to the physical electronic Hamiltonian

H in Eq. (1). Suppose we have solved Eq. (2) within a certain electronic-structure model and basis set and obtained a set of Siegert energies E_n and eigenfunctions $|\Psi_n\rangle$. Our aim is now to quantify the perturbation of E_n and $|\Psi_n\rangle$ by the CAP.

From Eq. (2) it follows that

$$\langle \Psi_n | H - i\eta W - E_t | \Psi_n \rangle = \langle \Psi_n | H - E_t | \Psi_n \rangle - i\eta \langle \Psi_n | W | \Psi_n \rangle = \Delta E_n \quad (13)$$

where $\Delta E_n = E_n - E_t$ and E_t is the real-valued threshold energy, i.e., the energy of the parent neutral molecule in the case of a TA. Eq. (13) can be decomposed into

$$\text{Re}(\Delta E_n) = \text{Re}\langle \Psi_n | H - E_t | \Psi_n \rangle + \text{Re}\langle -i\eta W \rangle_n \quad (14)$$

$$\text{Im}(\Delta E_n) = \text{Im}\langle \Psi_n | H | \Psi_n \rangle + \text{Im}\langle -i\eta W \rangle_n \quad (15)$$

where $\langle -i\eta W \rangle_n = -i\eta \langle \Psi_n | W | \Psi_n \rangle$ and c-normalization is assumed in Eqs. (13)–(15) and in the following.

If the CAP is a small perturbation, we expect

$$\left| \frac{\text{Re}\langle -i\eta W \rangle_n}{\text{Re}(\Delta E_n)} \right| \ll 1, \quad (16)$$

$$\left| \frac{\text{Im}\langle -i\eta W \rangle_n}{\text{Im}(\Delta E_n)} \right| \ll 1. \quad (17)$$

If Eq. (16) is fulfilled, we can rule out that the value computed for $\text{Re}(\Delta E_n)$ is an artifact of the CAP and not an approximation to the resonance position. Likewise, if Eq. (17) is fulfilled, the value computed for $\text{Im}(E_n)$ approximates the resonance half-width and is not an artifact of the CAP. Hence, $\text{Re}\langle -i\eta W \rangle_n / \text{Re}(\Delta E_n)$ and $\text{Im}\langle -i\eta W \rangle_n / \text{Im}(\Delta E_n)$ are functions quantifying perturbation due to the CAP. The closer both quantities are to zero, the more accurate the computed Siegert energy is expected to be.

We may define a single error function ξ from Eqs. (16) and (17) as

$$\xi := \sqrt{\left| \frac{\text{Re}\langle -i\eta W \rangle_n}{\text{Re}(\Delta E_n)} \right|^2 + \left| \frac{\text{Im}\langle -i\eta W \rangle_n}{\text{Im}(\Delta E_n)} \right|^2} \quad (18)$$

with $\text{Re}(\Delta E_n) \neq 0$ and $\text{Im}(\Delta E_n) \neq 0$. Here too, the closer ξ is to zero, the more accurate the computed Siegert energy is expected to be. We note that, in most molecular electronic-structure calculations, the contribution of the real part of the expectation value of the CAP to ξ is much smaller than that of the imaginary part, effectively reducing Eq. (18) to $\xi = |\text{Im}\langle -i\eta W \rangle_n / \text{Im}(\Delta E_n)|$.

Eq. (18) can be used to identify optimal values for arbitrary CAP parameters X according to

$$\min \xi(X) . \quad (19)$$

ξ can be computed as long as $\langle -i\eta W \rangle_n$ is defined, independent of which CAP parameters we seek to optimize. Eq. (19) thus constitutes a more general criterion than Eq. (7). Notably, optimization of η according to Eqs. (19) or (7) is not equivalent but we have not encountered any cases where the two criteria yield very dissimilar optimal CAP strengths, resonance positions and widths. The real benefit of Eq. (19) is, however, that the onset parameters \mathbf{r}^0 can be optimized as well.

We note that a deperturbed energy can be defined on the basis of Eq. (19) similar in spirit to Eq. (12):

$$\tilde{E}_n = E_n - \langle -i\eta W \rangle_n = \langle \Psi_n | H | \Psi_n \rangle \quad (20)$$

The deperturbed Siegert energy \tilde{E}_n is the expectation value of the physical Hamiltonian H with respect to the eigenfunction of H_{CAP} .

3 Computational details

We illustrate the usefulness of optimizing the CAP onset parameters by means of Eq. (19) by determining Siegert energies of the temporary anions of dinitrogen (${}^2\Pi_g$ state), ethylene (${}^2B_{2g}$ state), and formic acid (${}^2A''$ state). These shape resonances, especially N_2^- , have been studied several times using CAPs combined with different electronic-structure methods.^{32,34,36–52}

We note that for a box CAP, there is an infinite number of schemes how to vary the onset \mathbf{r}^0 . One may fix, for example, η , r_x^0, r_y^0 and vary r_z^0 . Or, alternatively, fix η , r_x^0, r_z^0 and vary r_y^0 . It is advisable, however, to choose a scheme that is compatible with the molecular point group. In this article, we use in most calculations a box CAP with the same onset in all directions, i.e., $r_x^0 = r_y^0 = r_z^0 = r^0$ where r^0 is the parameter we vary. This makes the comparison between results obtained with box and smooth Voronoi CAPs easy. r^0 is varied in steps of 0.1 a.u. unless indicated otherwise.

We use Hartree-Fock (HF) as well equation-of-motion electron-attachment coupled-cluster singles and doubles (EOM-EA-CCSD) theory,^{53,54} which were implemented for use with CAPs in the Q-Chem package.^{36,50,55} In the CAP-HF calculations, the core Hamiltonian guess together with the maximum-overlap method⁵⁶ is used to ensure convergence of the self-consistent field equations to the desired temporary anion state instead of some pseudocontinuum state. For the CAP-EOM-EA-CCSD calculations, we use two different approaches: In the first approach, referred to as “full CAP” in the following, CAP-HF and CAP-CCSD calculations are performed on the neutral molecule, followed by a CAP-EOM-EA-CCSD calculation on the anion. In the other approach, referred to as “projected CAP”, CAP-free HF, CCSD, and EOM-EA-CCSD calculations are performed, before H_{CAP} is constructed and diagonalized in the basis of EOM-CCSD states.^{39,51} The latter approach holds the advantage that the computationally expensive CCSD and EOM-CCSD calculations need to be carried out only once, whereas this has to be done anew for every value of the CAP parameters in the former approach.

All computations were done using the cc-pVTZ basis set augmented by a varying number

of diffuse s, p, and d shells on all atoms except hydrogen. The exponents of the additional shells are even-tempered with a spacing of 2 using the most diffuse shell of the cc-pVTZ basis with the same angular momentum as starting point. For all three TAs, the equilibrium structures of the corresponding neutral molecules as optimized at the HF/cc-pVTZ+3p or CCSD/cc-pVTZ+3p level were used; these structures are available from the Supporting Information. The integrals of the CAP over atomic orbitals were evaluated numerically on a Becke-type grid⁵⁷ of 99 radial points and 590 Lebedev angular points per radial point.^{36,50}

4 Results and discussion

4.1 CAP-HF calculations for the anion of dinitrogen

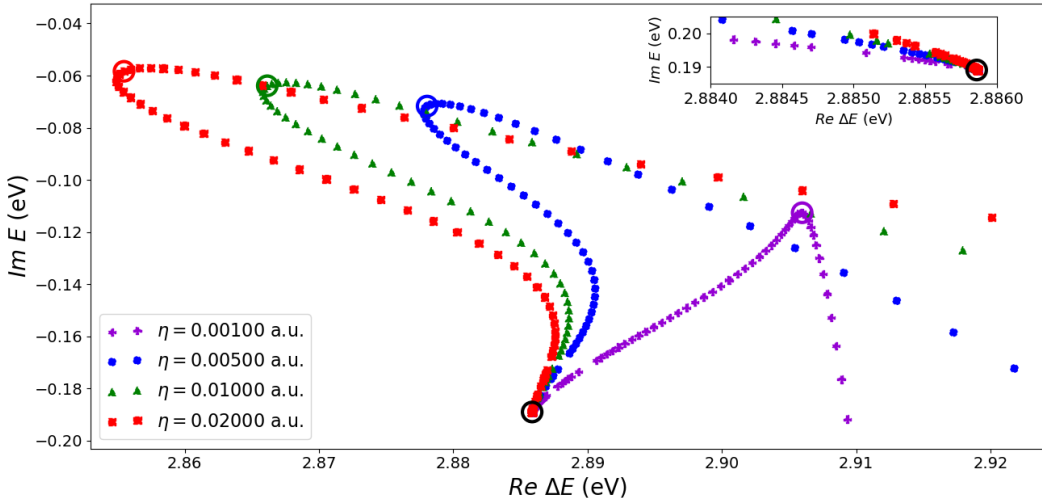


Figure 1: r^0 -Trajectories for the ${}^2\Pi_g$ resonance of N_2^- computed with box CAPs of different strengths η at the HF/cc-pVTZ+3p level of theory. Colored rings are put around points with minimum ξ , the two black rings indicate Siegert energies that are obtained over a wide range of large r^0 -values for all CAP strengths. The inset shows points with $\text{Im}(E) > 0$ that are also obtained with large r^0 -values.

Fig. 1 shows the distribution of CAP-HF energies in the complex plane computed for the ${}^2\Pi_g$ resonance of N_2^- with box CAPs with different onset parameters r^0 . The different colors indicate different CAP strengths η . It is obvious that these plots are different from the ones obtained by varying η at fixed r^0 . While η -trajectories begin at $\text{Im}(E) = 0$ for $\eta = 0$, which

corresponds to a CAP-free calculation, r^0 -trajectories such as the ones shown in Fig. 1 begin at some large imaginary energy that is obtained for $r^0 = 0$ and eventually reach $\text{Im}(E) = 0$, i.e., the CAP-free limit, once r^0 is so large that the CAP is invisible in the chosen basis set.

In Fig. 1, the points with the large spacing in the lower right correspond to low r^0 -values. As we increase r^0 , $\text{Im}(E)$ decreases until an abrupt turning point is reached, which corresponds to the optimal r^0 -values according to Eq. (19), i.e., a minimum in ξ . Increasing r^0 further does not yield the CAP-free limit $\text{Im}(E) = 0$ immediately; instead, all r^0 -trajectories converge to the same CAP-HF energy for all values of r^0 between ca. 8 and 20 a.u. This unphysical energy is indicated by a black circle in Fig. 1. Only with even larger r^0 , $\text{Im}(E) = 0$ is obtained. Notably, the r^0 -trajectories obtained with CAP strengths of 0.02 a.u., 0.01 a.u., and 0.005 a.u. look very similar, whereas the one obtained with 0.001 a.u. differs significantly, suggesting that this value for η is insufficient.

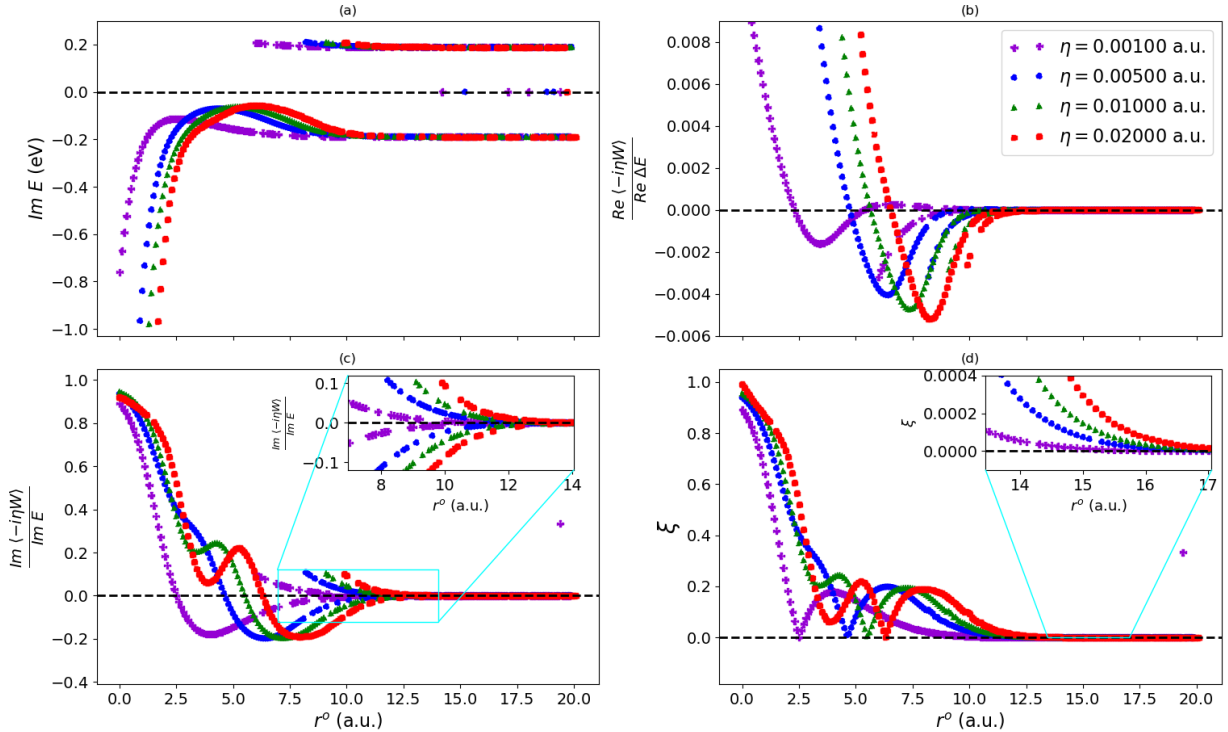


Figure 2: Further analysis of the r^0 -trajectories from Fig. 1: (a) imaginary energy, (b) real part of the expectation value of the CAP, (c) imaginary part of the expectation value of the CAP, and (d) error function ξ , all as a function of r^0 .

This is confirmed by the upper left part of Tab. 1, which shows resonance positions and

widths as well as the optimal r^0 and ξ values for the CAP-HF calculations from Fig. 1. If the computation with $\eta = 0.001$ a.u. is neglected, the variations in ΔE and Γ do not exceed 0.003 eV. By comparison, in CAP-EOM-EA-CCSD calculations in which η is optimized, variations of r^0 by 0.5 a.u. can lead to differences of 0.05 eV in ΔE and Γ .³⁶ We also note that the values for the deperturbed resonance position and width in Tab. 1, computed using Eq. (20), are almost identical to the original values, which is different from the approach where η is optimized. Here, the first-order correction according to Eq. (12) can make a significant impact. Furthermore, Tab. 1 shows that higher values for η mandate a larger CAP-free region.

Results from CAP-HF calculations with smooth Voronoi CAPs instead of box CAPs are reported in the second part of Tab. 1. The computed resonance positions and widths are almost identical but the optimal r^0 -values as determined according to Eq. (19) are consistently larger by about 1 a.u. as compared to the box CAP calculations. The underlying r^0 -trajectories are reported in the Supporting Information and look very similar to those from Fig. 1. From Tab. 1, it is evident that CAP-HF overestimates the resonance position and underestimates the resonance width of N_2^- . This can be attributed to the neglect of electron correlation.⁸ However, the CAP-HF values in Tab. 1 are in good agreement with CAP-HF calculations based on Eq. (7) that yielded 2.79 eV and 0.13 eV for the resonance position and width using a somewhat bigger basis set.⁸

To analyse the r^0 -trajectories from Fig. 1 further, we report in Fig. 2 several additional quantities. Panel (a) shows the imaginary energy as a function of r^0 . This plot illustrates that the same CAP-HF energy is obtained between 8 a.u. and 20 a.u. for all four values of η that we used. Moreover, a CAP-HF calculation run with such r^0 -value can also converge to an energy with the same real part but positive imaginary part or, as a third solution, to the same real part and $\text{Im}(E) = 0$. The latter energy is identical to the one obtained in the corresponding CAP-free calculation. This behavior is clearly unphysical and likely caused by the non-linear parameterization of the CAP-HF equations, which do not necessarily need

to have the same solution manifold as Eq. (2).

Panels (b) and (c) of Fig. 2 show the contribution of the expectation value of the CAP to the overall values of $\text{Re}(\Delta E)$ and $\text{Im}(E)$, respectively. As motivated in Sec. 2.2, these functions quantify the perturbation of $\text{Re}(\Delta E)$ and $\text{Im}(E)$ by the CAP. For all four CAP strengths we tested, there are two values of r^0 in the range 2–8 a.u. where $\text{Re}\langle i\eta W \rangle$ and $\text{Im}\langle i\eta W \rangle$, respectively, vanish, meaning that there is no perturbative contribution to $\text{Re}(\Delta E)$ and $\text{Im}(E)$. Interestingly, also the unphysical solution obtained at 8 a.u. $< r^0 < 20$ a.u. is characterized by vanishing $\text{Re}\langle i\eta W \rangle$, $\text{Im}\langle i\eta W \rangle$, and ξ .

Unfortunately, the physically meaningful zeros of $\text{Re}\langle i\eta W \rangle$ and $\text{Im}\langle i\eta W \rangle$ occur at different values of r^0 so that ξ computed using Eq. (18) has multiple minima as displayed in panel (d) of Fig. 2. This is akin to what one observes if η is optimized according to Eq. (7): Although $d\text{Re}(E)/d\eta$ and $d\text{Im}(E)/d\eta$ usually vanish at some η , they do not vanish simultaneously giving rise to multiple minima in $\eta dE/d\eta$. Although it has been argued that the evaluation of ΔE and Γ with different CAP parameters may improve resonance positions and widths,³⁵ this is rarely done and we believe it is also not advisable in the framework of the present work. Consequently, we use the global minimum of ξ for the values in Tab. 1 and the following tables.

4.2 CAP-EOM-EA-CCSD calculations for the anion of dinitrogen

Fig. 3 shows r^0 -trajectories for the ${}^2\Pi_g$ resonance of N_2^- computed with CAP-EOM-EA-CCSD and different CAP strengths. Resonance positions and widths from these calculations are reported in the third part of Tab. 1. Similar to Fig. 1, the data points in the lower right part of Fig. 3 correspond to low r^0 -values. Upon increasing r^0 , the complex energy stabilizes, eventually a turning point is reached, and ξ assumes its minimum value. A striking difference to Fig. 1 is that the r^0 -trajectories converge to the CAP-free limit ($\text{Im}(E) = 0$) straight away after the turning point; we did not encounter any unphysical solution of the CAP-EOM-EA-CCSD equations at large r^0 . This is no surprise because the CAP-EOM-

Table 1: Vertical attachment energies ΔE and resonance widths Γ in eV for the ${}^2\Pi_g$ resonance of N_2^- computed with different CAP methods and the cc-pVTZ+3p basis set. $\Delta\tilde{E}$ and $\tilde{\Gamma}$ are the deperturbed vertical attachment energy and resonance width according to Eq. (20). Optimal values for r^0 according to Eq. (19) and corresponding values of ξ are given in a.u.

η	r_{opt}^0	$\xi(r_{\text{opt}}^0)$	ΔE	$\Delta\tilde{E}$	Γ	$\tilde{\Gamma}$	r_{opt}^0	$\xi(r_{\text{opt}}^0)$	ΔE	$\Delta\tilde{E}$	Γ	$\tilde{\Gamma}$
			box CAP/HF				projected box CAP/EOM-EA-CCSD, $n = 2$ ^a					
0.001	2.5	0.0006	2.906	2.908	0.225	0.225	2.600	0.3146	2.754	2.856	0.306	0.211
0.005	4.6	0.0100	2.878	2.876	0.143	0.142	4.300	0.0243	2.669	2.703	0.238	0.233
0.010	5.5	0.0064	2.866	2.864	0.128	0.127	5.188	0.0080	2.649	2.670	0.201	0.201
0.020	6.3	0.0021	2.856	2.852	0.117	0.117	6.042	0.0053	2.633	2.647	0.173	0.173
all	big	0.0000	2.886	2.886	0.378	0.378						
			smooth Voronoi-CAP/HF				projected box CAP/EOM-EA-CCSD, $n = 5$ ^a					
0.001	2.9	0.0102	2.906	2.907	0.217	0.215	2.5	0.4292	2.767	2.856	0.351	0.201
0.005	5.7	0.0026	2.875	2.874	0.134	0.135	4.5	0.0129	2.667	2.702	0.296	0.296
0.010	6.7	0.0053	2.862	2.861	0.116	0.115	5.3	0.0215	2.636	2.653	0.262	0.257
0.020	7.6	0.0019	2.850	2.849	0.102	0.102	6.2	0.0385	2.606	2.621	0.225	0.233
all	big	0.0000	2.886	2.886	0.378	0.378						
			box CAP/EOM-EA-CCSD				projected box CAP/EOM-EA-CCSD, $n = 9$ ^a					
0.001	2.4	0.4304	2.767	2.850	0.368	0.210	2.4	0.4327	2.767	2.850	0.365	0.208
0.005	4.5	0.0098	2.672	2.699	0.306	0.306	4.5	0.0140	2.671	2.700	0.303	0.301
0.010	5.3	0.0089	2.642	2.647	0.273	0.271	5.4	0.0315	2.636	2.654	0.268	0.276
0.020	6.1	0.0080	2.616	2.613	0.238	0.239	6.2	0.0102	2.607	2.617	0.237	0.239
			smooth Voronoi-CAP/EOM-EA-CCSD									
0.001	2.9	0.3664	2.764	2.847	0.341	0.216						
0.005	5.4	0.0059	2.662	2.677	0.281	0.281						
0.010	6.4	0.0174	2.627	2.630	0.236	0.240						
0.020	7.2	0.0346	2.601	2.595	0.199	0.192						
Reference value ⁵⁸			2.32		0.41							

^a Using the n lowest-lying right and left EOM-EA-CCSD eigenstates as basis.

CC Hamiltonian is a similarity transform of H_{CAP} so that, in contrast to CAP-HF theory, additional solutions do not exist.

The differences between CAP-EOM-EA-CCSD and CAP-HF are also evident from Fig. 4, which shows for CAP-EOM-EA-CCSD the same quantities that are shown for CAP-HF in Fig. 2. The imaginary energy in panel (a) reaches the CAP-free limit between 10 and 12 a.u. and from panel (c) it is evident that $\text{Im}(E)$ almost exclusively consists of $\text{Im}\langle i\eta W \rangle$ at large r^0 -values. This implies that the deperturbed imaginary energy according to Eq. (20) is practically zero, i.e., the CAP mainly acts as a perturbation at large r^0 and the resonance position and width must be evaluated at lower r^0 .

Table 2: Vertical attachment energies ΔE and resonance widths Γ in eV for the ${}^2\Pi_g$ resonance of N_2^- evaluated using Eq. (7) at fixed r^0 , using Eq. (19) at fixed r^0 , and using Eq. (19) at fixed η . All computations were done with box-CAP-EOM-EA-CCSD and the aug-cc-pVTZ+6s6p6d basis set. $\Delta\tilde{E}$ and $\tilde{\Gamma}$ are the deperturbed vertical attachment energy and resonance width according to Eqs. (12) or (20). Values of η , r^0 , and ξ are given in a.u.

r^0	η	ξ	ΔE	$\Delta\tilde{E}$	Γ	$\tilde{\Gamma}$
Determined from an η -trajectory using Eq. (7)						
2.765/2.765/4.881 ^a	0.00360 ^b	0.1716	2.570	2.571	0.361	0.423
Determined from an η -trajectory using Eq. (19)						
2.765/2.765/4.881 ^a	0.00420 ^b	0.0172	2.571	2.559	0.356	0.362
Determined from an r^0 -trajectory using Eq. (19)						
1.6/1.6/1.6 ^b	0.00100 ^a	0.0195	2.616	2.613	0.655	0.642
3.6/3.6/3.6 ^b	0.00500 ^a	0.0146	2.571	2.548	0.319	0.323
4.4/4.4/4.4 ^b	0.01000 ^a	0.0274	2.552	2.524	0.257	0.251
5.3/5.3/5.3 ^b	0.02000 ^a	0.0161	2.526	2.502	0.204	0.207
Reference value ⁵⁸			2.32		0.41	

^a Fixed. ^b Optimized.

Interestingly, there are several r^0 -values for which $\text{Im}\langle i\eta W \rangle$ vanishes in the CAP-EOM-EA-CCSD calculations, whereas this happens for exactly one r^0 -value in the CAP-HF calculations reported in Fig. 2. The corresponding real part of the expectation value, $\text{Re}\langle i\eta W \rangle$, which is displayed in panel (b) of Fig. 4, behaves similarly for CAP-EOM-EA-CCSD and CAP-HF. Owing to the behavior of $\text{Im}\langle i\eta W \rangle$, ξ shown in panel (d) of Fig. 4 has up to four minima.

The CAP-EOM-EA-CCSD resonance positions and widths reported in the third part of Tab. 1 are evaluated at the global minimum of ξ . These values show a more pronounced dependence on η than the CAP-HF values in the upper part of the same table, while the optimal r^0 is very similar for CAP-HF and CAP-EOM-EA-CCSD. ΔE and Γ evaluated with CAP strengths of 0.005 a.u. and 0.02 a.u. differ by up to 0.05 eV and 0.08 eV, respectively. This is akin to the sensitivity toward the CAP onset observed in CAP-EOM-EA-CCSD calculations in which η is optimized³⁶ and demonstrates that choosing η correctly is important in our approach where r^0 is optimized. By comparing the values of ξ in Tab. 1, we conclude that 0.02 a.u. is the best among the four CAP strengths we used. We further note that the correction from Eq. (20) generally makes a negligible impact on positions and

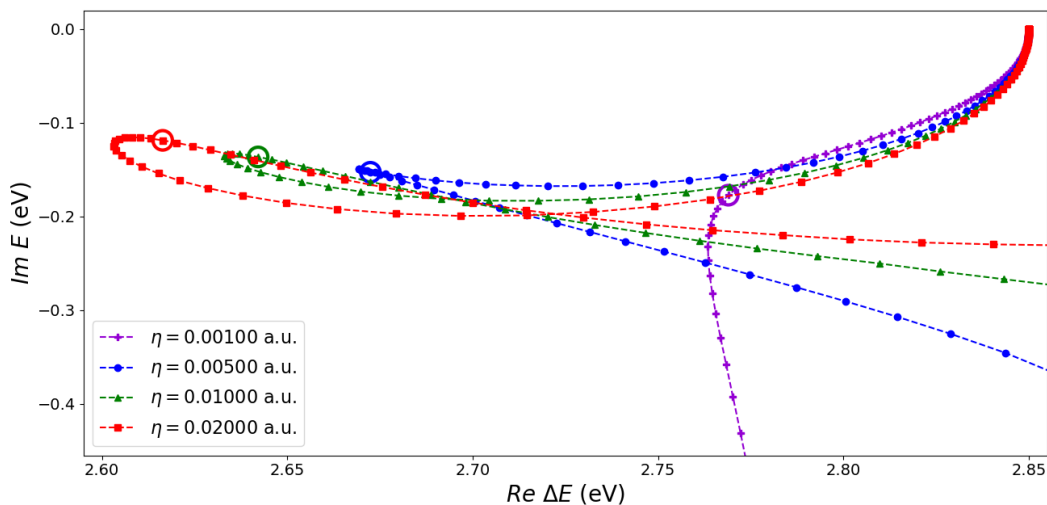


Figure 3: r^0 -Trajectories for the ${}^2\Pi_g$ resonance of N_2^- computed with box CAPs of different strengths η at the EOM-EA-CCSD/cc-pVTZ+3p level of theory. Colored rings are put around points with minimum ξ .

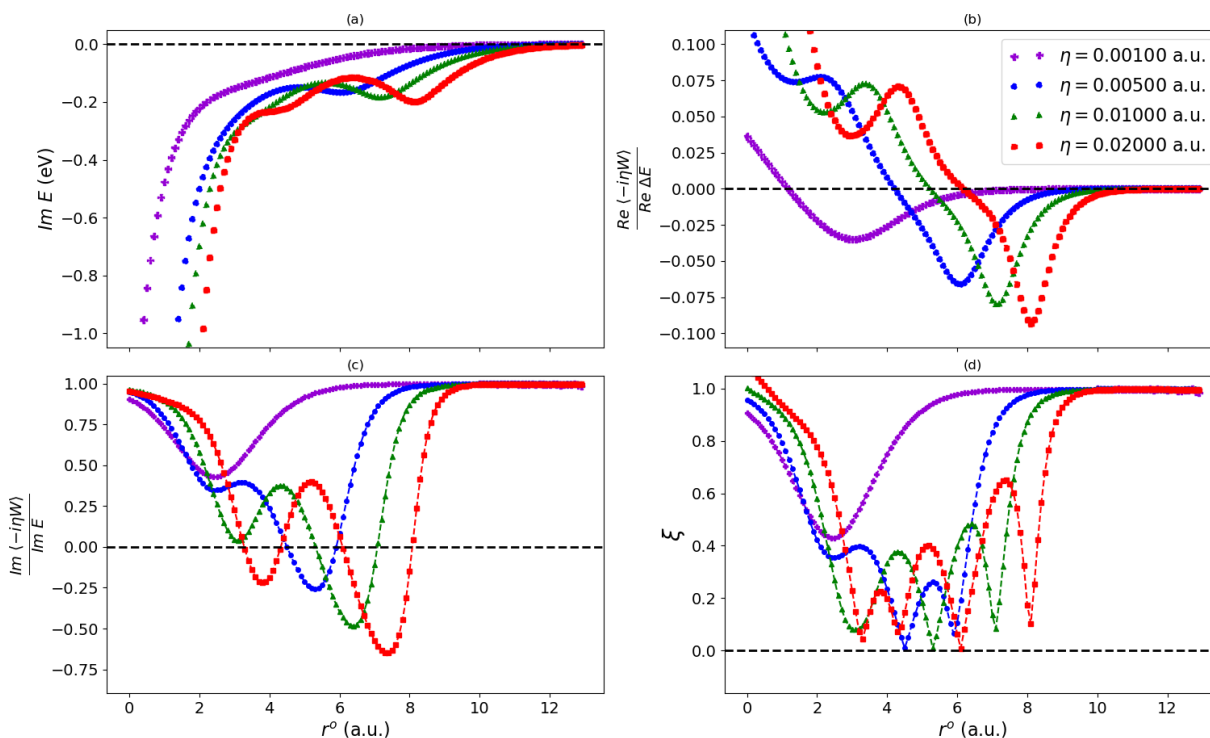


Figure 4: Further analysis of the r^0 -trajectories from Fig. 3: (a) imaginary energy, (b) real part of the expectation value of the CAP, (c) imaginary part of the expectation value of the CAP, and (d) error function ξ , all as a function of r^0 .

widths except for $\eta = 0.001$ a.u. Together with the large value of ξ , this indicates that 0.001 a.u. is an insufficient CAP strength.

The fourth part of Tab. 1 reports resonance energies and widths computed with CAP-EOM-EA-CCSD and a smooth Voronoi CAP instead of box CAP. The corresponding r^0 -trajectories are reported in the Supporting Information and look very similar to those from Fig. 3. As we discussed for CAP-HF, optimal r^0 -values are bigger by about 1 a.u. in calculations with a smooth Voronoi CAP compared to the box CAP. The differences in the resonance positions and widths computed with box CAP and smooth Voronoi CAP amount to up to 0.02 eV and are thus somewhat larger than in CAP-HF calculations.

On the right hand side of Tab. 1, we show results from projected CAP-EOM-EA-CCSD calculations.⁵¹ The corresponding r^0 -trajectories are available in the Supporting Information and look again similar to those from Fig. 3. Using 2 CAP-free EOM-EA-CCSD eigenstates as basis, the resonance positions computed with the projected approach deviate by no more than 0.02 eV from the values obtained with full CAP-EOM-EA-CCSD, but the resonance width is systematically underestimated by up to 0.07 eV. Using 5 EOM-EA-CCSD eigenstates as basis reduces the deviation in the width to less than 0.02 eV, and in a basis of 9 states the width is identical to values from full CAP-EOM-EA-CCSD up to 0.005 eV.

Notably, all CAP-EOM-EA-CCSD results in Table 1 differ substantially from the reference value, which was obtained from a model fitted to the experimental cross section of $\text{N}_2\text{-}e^-$ scattering.⁵⁸ This can likely be attributed to the use of the relatively small cc-pVTZ+3p basis set. Previous CAP-EOM-EA-CCSD calculations demonstrated that the use of a quadruple- ζ or quintuple- ζ basis, the inclusion of more than three diffuse p -shells, and especially the inclusion of diffuse d -shells bring the position and width in better agreement with the reference value.^{36,51,59}

To corroborate this point and to directly compare results from Eqs. (7) and (19), we carried out additional CAP-EOM-EA-CCSD calculations using an aug-cc-pVTZ+6s6p6d basis set, which is available from the Supporting Information. These results are summarized in

Table 2. Evidently, the use of the larger basis set improves the resonance position significantly by ca. 0.1 eV compared to Table 1. It is furthermore apparent that optimization of the CAP onset r^0 at fixed CAP strength η and the opposite approach yield very similar resonance positions if the respective fixed parameter is chosen well. The resonance width is improved by the bigger basis set as well, but here a significant deviation of ca. 0.04 eV between optimization of η and optimization of r^0 remains. Lastly, the results for Γ in Table 1 also illustrate that Eqs. (7) and (19) are not numerically equivalent although the differences amount to no more than 0.005 eV.

4.3 Anion of ethylene

As a second test case, we studied the ${}^2B_{2g}$ resonance of $C_2H_4^-$. Tab. 3 summarizes our results for the position and width of this resonance computed at the CAP-HF and CAP-EOM-EA-CCSD levels of theory. The corresponding r^0 -trajectories are available in the Supporting Information. These trajectories look by and large similar to those of N_2^- that we discussed in Secs. 4.1 and 4.2 with the following important differences: Firstly, we did not encounter any unphysical solutions of the CAP-HF equations at large r^0 -values. Rather, the r^0 -trajectories directly reach the CAP-free limit. Secondly, ξ has multiple minima also in the CAP-HF case and, lastly, all CAP-HF trajectories show a discontinuity associated with an abrupt change in the character of the wave function.

From the large ξ -values in Tab. 3, it is clear that 0.001 a.u. is too weak a CAP strength to describe the resonance state. Similar to N_2^- (Tab. 1), increasing the CAP strength from 0.005 a.u. to 0.02 a.u. yields larger optimal r^0 -values. An interesting difference to N_2^- is, however, that the optimal r^0 -values do not differ much between calculations with box CAP and smooth Voronoi CAP.

The resonance positions obtained with CAP-EOM-EA-CCSD and CAP strengths of 0.005, 0.01, and 0.02 a.u. differ by no more than 0.06 eV and are also in good agreement with previous CAP-EOM-EA-CCSD calculations in which η was optimized at fixed

Table 3: Vertical attachment energies ΔE and resonance widths Γ in eV for the ${}^2B_{2g}$ resonance of $C_2H_4^-$ computed with different CAP methods and the cc-pVTZ+3p basis set. $\Delta\tilde{E}$ and $\tilde{\Gamma}$ are the deperturbed vertical attachment energy and resonance width according to Eq. (20). Optimal values for r^0 according to Eq. (19) and corresponding values of ξ are given in a.u.

η	r_{opt}^0	$\xi(r_{\text{opt}}^0)$	ΔE	$\Delta\tilde{E}$	Γ	$\tilde{\Gamma}$	r_{opt}^0	$\xi(r_{\text{opt}}^0)$	ΔE	$\Delta\tilde{E}$	Γ	$\tilde{\Gamma}$
			box CAP/HF				projected box CAP/EOM-EA-CCSD, $n = 2$ ^a					
0.001	2.4	0.1546	2.823	2.759	0.679	0.575	4.0	0.2022	2.189	2.303	0.340	0.273
0.005	6.4	0.0473	2.674	2.757	0.550	0.531	6.0	0.0335	2.102	2.134	0.247	0.255
0.010	6.9	0.0194	2.537	2.563	0.526	0.517	6.8	0.0362	2.082	2.098	0.206	0.199
0.020	7.7	0.0073	2.464	2.475	0.450	0.448	7.7	0.0083	2.065	2.075	0.164	0.165
			smooth Voronoi CAP/HF				projected box CAP/EOM-EA-CCSD, $n = 5$ ^a					
0.001	2.0	0.1159	2.821	2.758	0.641	0.568	3.9	0.3558	2.209	2.309	0.409	0.264
0.005	6.5	0.0196	2.602	2.653	0.547	0.547	6.1	0.0292	2.095	2.116	0.330	0.321
0.010	7.3	0.0093	2.493	2.509	0.472	0.475	7.0	0.0362	2.061	2.069	0.277	0.267
0.020	8.1	0.0161	2.425	2.429	0.377	0.371	7.9	0.0048	2.032	2.037	0.225	0.224
			box CAP/EOM-EA-CCSD				projected box CAP/EOM-EA-CCSD, $n = 9$ ^a					
0.001	3.8	0.3603	2.212	2.301	0.422	0.271	3.8	0.3613	2.212	2.301	0.421	0.270
0.005	6.2	0.0233	2.096	2.119	0.337	0.344	6.2	0.0244	2.095	2.119	0.335	0.342
0.010	7.1	0.0156	2.059	2.066	0.286	0.290	7.1	0.0171	2.059	2.067	0.283	0.288
0.020	7.9	0.0341	2.031	2.030	0.240	0.232	7.9	0.0326	2.031	2.031	0.238	0.230
			smooth Voronoi CAP/EOM-EA-CCSD									
0.001	3.9	0.3228	2.209	2.308	0.400	0.272						
0.005	6.5	0.0203	2.081	2.095	0.308	0.314						
0.010	7.5	0.0025	2.043	2.045	0.250	0.250						
0.020	8.4	0.0224	2.014	2.012	0.199	0.195						
Experiment ^{60,61}			1.8		0.7							

^a Using the n lowest-lying right and left EOM-EA-CCSD eigenstates as basis.

CAP onset.^{36,51} In Ref. 36, the resonance position of $C_2H_4^-$ was computed to be 2.09 eV and 1.99 eV using the aug-cc-pVTZ+3s3p3d and aug-cc-pVQZ+3s3p3d basis sets, respectively. Notably, changing the CAP onset by 0.5 a.u. led to changes of at most 0.02 eV in the resonance position of $C_2H_4^-$, i.e., the results from Ref. 36 are less sensitive than those obtained with the present approach. CAP-HF yields considerably higher resonance positions than CAP-EOM-EA-CCSD, which is similar to N_2^- (Tab. 1) and can again be attributed to the neglect of electron correlation. Somewhat surprisingly, however, η has a bigger impact on the resonance positions in the CAP-HF calculations.

The CAP-EOM-EA-CCSD resonance widths computed with CAP strengths of 0.005 a.u.,

0.01 a.u., and 0.02 a.u. differ by up to 0.10 eV and are thus also more sensitive than in the approach where the CAP strength is optimized at fixed onset. In Ref. 36, a change of 0.5 a.u. in the CAP onset led to changes of at most 0.05 eV in the width of C_2H_4^- . Also, the widths obtained with the present approach are smaller by 0.10–0.20 eV than those obtained with the aug-cc-pVTZ+3s3p3d basis and fixed onset in Ref. 36. Moreover, CAP-HF yields a larger resonance width than CAP-EOM-EA-CCSD according to Tab. 3, which is in disagreement not only with the results for N_2^- but also with previous results for other molecules.^{8,62}

Using ξ as a quality measure, our best values for the resonance position and width are 2.04 eV and 0.25 eV, respectively. With respect to the value extracted from C_2H_4-e^- scattering experiments,^{60,61} the resonance is thus 0.24 eV too high in energy. The width is significantly underestimated with respect to the experimental value of 0.7 eV. In view of the results from Ref. 36, these discrepancies can be ascribed at least partly to our use of the relatively small cc-pVTZ+3p basis set.

We note that the correction from Eq. (20) is negligible as long as an adequate CAP strength is used, indicated by a small value of ξ . Differences between box and Voronoi CAPs are very small in CAP-EOM-EA-CCSD calculations but significant in CAP-HF calculations with the same η . If one compares results computed with those η -values that yield the smallest ξ (0.02 a.u. for box CAP, 0.01 a.u. for Voronoi CAP), the agreement becomes much better for CAP-HF too.

Regarding projected CAP-EOM-EA-CCSD, Tab. 3 shows that a basis of two CAP-free EOM-CCSD states is already sufficient to describe the position of C_2H_4^- accurately, whereas the width is underestimated by up to 0.08 eV. With a basis of 5 states, the deviation in the width goes down to 0.02 eV and with a basis of 9 states, the widths are essentially identical to those from full CAP-EOM-EA-CCSD.

Table 4: Vertical attachment energies ΔE and resonance widths Γ in eV for the ${}^2A''$ resonance of HCOOH^- computed with different CAP methods and the cc-pVTZ+3p basis set. $\Delta\tilde{E}$ and $\tilde{\Gamma}$ are the deperturbed vertical attachment energy and resonance width according to Eq. (20). Optimal values for r^0 according to Eq. (19) and corresponding values of ξ are given in a.u.

η	r_{opt}^0	$\xi(r_{\text{opt}}^0)$	ΔE	$\Delta\tilde{E}$	Γ	$\tilde{\Gamma}$	r_{opt}^0	$\xi(r_{\text{opt}}^0)$	ΔE	$\Delta\tilde{E}$	Γ	$\tilde{\Gamma}$
	box CAP/HF/ <i>cis</i> -conformer						projected box CAP/EOM-EA-CCSD, $n = 2$ ^a					
0.001	4.1	0.0059	2.994	2.976	0.490	0.490	<i>cis</i> -conformer					
0.005	6.6	0.0042	3.002	2.989	0.513	0.513	7.5	0.7206	1.825	1.921	0.597	0.168
0.010	7.5	0.0047	3.006	2.994	0.525	0.524	8.8	0.5517	1.813	1.913	0.441	0.199
0.020	8.2	0.0034	3.013	3.002	0.536	0.536	9.8	0.3517	1.793	1.893	0.372	0.243
all	big	0.0000	2.952	2.952	0.477	0.477						
all	big	0.0000	2.710	2.710	0.044	0.044						
	smooth Voronoi CAP/HF/ <i>cis</i> -conformer						projected box CAP/EOM-EA-CCSD, $n = 6$ ^a					
0.001	4.9	0.0053	2.990	2.974	0.486	0.486	<i>cis</i> -conformer					
0.005	7.1	0.0040	3.011	3.000	0.517	0.516	3.5	0.0365	2.656	2.753	0.700	0.702
0.010	7.9	0.0038	3.020	3.011	0.532	0.533	4.1	0.0243	2.617	2.675	0.584	0.578
0.020	8.8	0.0030	3.026	3.017	0.543	0.543	4.8	0.0287	2.588	2.628	0.501	0.513
all	big	0.0000	2.952	2.952	0.477	0.477						
all	big	0.0000	2.710	2.710	0.044	0.044						
	box CAP/EOM-EA-CCSD/ <i>cis</i> -conformer						box CAP/EOM-EA-CCSD/ <i>trans</i> -conformer					
0.001	2.7	0.5095	1.794	1.957	2.021	1.008	1.9	0.3244	2.305	1.968	1.253	0.890
0.005	3.2	0.0287	2.703	2.699	0.921	0.895	3.7	0.0428	2.367	2.286	0.515	0.528
0.010	3.7	0.0265	2.696	2.651	0.754	0.770	4.2	0.0384	2.383	2.293	0.439	0.436
0.020	4.2	0.0447	2.694	2.639	0.614	0.639	4.6	0.0393	2.408	2.319	0.390	0.395
	smooth Voronoi CAP/EOM-EA-CCSD/ <i>cis</i> -conformer											
0.001	2.7	0.5025	1.813	1.927	1.812	0.909						
0.005	2.5	0.0356	2.723	2.661	0.755	0.776						
0.010	3.0	0.0322	2.737	2.653	0.629	0.635						
0.020	3.5	0.0398	2.747	2.659	0.523	0.510						
Experiment ⁶³			1.73									

^a Using the n lowest-lying right and left EOM-EA-CCSD eigenstates as basis.

4.4 Anion of formic acid

As a third test case, we studied the ${}^2A''$ resonance of the *cis*-conformer of HCOOH^- . Positions and widths computed for this resonances with CAP-HF and CAP-EOM-EA-CCSD are summarized in Tab. 4. The corresponding r^0 -trajectories are available in the Supporting Information. The basic structure of these trajectories is the same as for N_2^- and C_2H_4^- . At large r^0 -values above 10 a.u., CAP-HF yields unphysical solutions similar to those discussed for N_2^- in Sec. 4.1. Also, discontinuities are present in some CAP-EOM-EA-CCSD trajecto-

ries and ξ has multiple minima in these cases. The resonance positions and widths reported for HCOOH^- in Tab. 4 are evaluated at the global minimum of ξ .

Similar to the previously discussed molecules, 0.001 a.u. is again too weak a CAP strength in CAP-EOM-EA-CCSD calculations. Higher CAP strengths between 0.005 a.u. and 0.02 a.u. produce almost identical resonance positions with the variation not exceeding 0.02 eV, while the switch from box CAP to Voronoi CAP changes the position by no more than 0.04 eV. The impact of the correction from Eq. (20) is in some cases a little larger than for N_2^- and C_2H_4^- but does not exceed 0.09 eV. CAP-HF yields significantly higher resonance positions than CAP-EOM-EA-CCSD owing to the neglect of electron correlation.

Using ξ as a quality measure, our best value for the resonance position of HCOOH^- is 2.65 eV. An assessment of this value is complicated by the fact that previous theoretical investigations focused on the *trans*-conformer of HCOOH , which is more stable than the *cis*-conformer by 0.17 eV.⁶⁴ We therefore conducted additional CAP-EOM-EA-CCSD calculations on the *trans*-conformer, which are reported in the lower right section of Table 4. Our best value for the resonance position of the *trans*-conformer is 2.29 eV, i.e., 0.36 eV less than for the *cis*-conformer. This confirms previous results: With CAP-EOM-EA-CCSD, fixed CAP onset and optimized η , a value of 2.287 eV was computed for the resonance position at the *trans*-structure,⁴⁶ while scattering calculations with the complex Kohn method yielded a position of 1.9 eV.⁶⁵ Electron transmission spectroscopy suggested a value of 1.73 eV for the position of HCOOH^- ,⁶³ while the dissociative electron attachment cross section has a peak at 1.25 eV.⁶⁶ We also mention electron energy loss spectroscopy on HCOOH ⁶⁷ and measurements of the differential cross section in $\text{HCOOH}-e^-$ scattering.⁶⁸ Moreover, there is evidence that the anion potential energy surface is flatter than that of neutral HCOOH .^{46,65}

Regarding the resonance width, Tab. 4 demonstrates that technical details make a sizable impact, especially in the case of CAP-EOM-EA-CCSD. Widths of the *cis*-conformer obtained with CAP strengths of 0.005 a.u. and 0.02 a.u. differ by up to 0.30 eV even though ξ is of the same order of magnitude. Also, the width changes by up to 0.17 eV when going from

box CAP to Voronoi CAP. The correction from Eq. (20), however, has a surprisingly small impact on the width not exceeding 0.03 eV. With CAP-HF the resonance is significantly narrower than with CAP-EOM-EA-CCSD similar to what we found for N_2^- .

Our best values for the resonance widths of the *cis*- and *trans*-conformers are 0.770 eV and 0.436 eV, respectively. The latter value is considerably larger than the resonance width of 0.27 eV computed for the *trans*-conformer⁴⁶ with CAP-EOM-EA-CCSD, fixed CAP onset and optimized η . We add that the complex Kohn method yielded a value of 0.2 eV for the resonance width at the *trans*-structure.⁶⁵ Notwithstanding the large variations among the Γ -values in Tab. 4, our results suggest that the *cis*-conformer has a larger resonance width than the *trans*-conformer.

As concerns projected CAP-EOM-EA-CCSD, Tab. 4 demonstrates that a basis of two states is not adequate for either the position or the width of HCOOH^- . Even with six states as basis, the discrepancy between full and projected CAP-EOM-EA-CCSD still amounts to 0.05–0.10 eV for the position and 0.11–0.22 eV for the width.

4.5 Role of diffuse basis functions

It is well established that the description of TAs by means of CAP methods mandates the use of customized basis sets.⁸ A possible strategy is to augment correlation consistent basis sets^{69,70} by additional shells of diffuse functions. Whereas one can anticipate that *p*-shells are most important to describe π^* -resonances such as the ones studied here, the number of shells required for convergence varies from case to case.

In Tab. 5, we report resonance positions and widths for N_2^- and C_2H_4^- that were computed with different numbers of diffuse shells included in the basis set. For N_2^- , the additional shells are even tempered, whereas this was not possible for C_2H_4^- because of linear dependencies in the basis. For the latter molecule, the exponents of the additional shells are available in the Supporting Information.

The upper section of Tab. 5 shows that basis set convergence is achieved relatively easily

Table 5: Vertical attachment energies ΔE and resonance widths Γ in eV for the ${}^2\Pi_g$ resonance of N_2^- and the ${}^2\text{B}_{2g}$ resonance of C_2H_4^- computed using different basis sets cc-pVTZ+ np and a CAP strength of 0.005 a.u. $\Delta\tilde{E}$ and $\tilde{\Gamma}$ are the deperturbed vertical attachment energy and resonance width according to Eq. (20). Optimal values for r^0 according to Eq. (19) and corresponding values of ξ are given in a.u.

n	r_{opt}^0	$\xi(r_{\text{opt}}^0)$	ΔE	$\Delta\tilde{E}$	Γ	$\tilde{\Gamma}$
N_2^- / box CAP / HF						
3	4.6	0.0100	2.878	2.876	0.143	0.142
6	7.8	0.0046	2.849	2.847	0.285	0.286
8	7.8	0.0003	2.848	2.847	0.282	0.282
12	7.8	0.0010	2.848	2.847	0.281	0.281
Reference value ⁵⁸			2.32		0.41	
C_2H_4^- / smooth Voronoi CAP / HF ^a						
2	2.7	0.0290	2.987	2.901	0.742	0.743
3	5.6	0.0105	2.791	2.818	0.381	0.380
4	4.1	0.0076	2.891	2.872	0.433	0.435
C_2H_4^- / smooth Voronoi CAP/EOM-EA-CCSD ^a						
2	2.2	0.0927	2.587	2.368	1.048	1.008
3	5.3	0.0022	2.218	2.222	0.292	0.291
4	4.3	0.0230	2.311	2.270	0.402	0.396
5	4.1	0.0216	2.332	2.283	0.422	0.423
6	3.9	0.0286	2.353	2.293	0.446	0.440
7	3.8	0.0300	2.364	2.297	0.464	0.459
8	3.8	0.0288	2.364	2.297	0.464	0.461
Experiment ^{60,61}			1.8		0.7	

in CAP-HF calculations on N_2^- . The resonance position is accurate to 0.03 eV already with three extra p -shells; and with six of them the resonance width is converged as well. The fact that more than six extra p -shells are not needed is also apparent from the r^0 -trajectories reported in the Supporting Information, which barely change upon enlarging the basis further.

It is noteworthy that even in a basis set with twelve additional p -shells where the smallest exponent is of the order of 10^{-5} , convergence of the CAP-HF equations to the desired solution can still be achieved for N_2^- . This is not the case for C_2H_4^- where we were unable to find the CAP-HF solution corresponding to the ${}^2\text{B}_{2g}$ resonance when more than four diffuse p -shells were present. The middle section of Tab. 5 illustrates that the position and width of C_2H_4^-

are not yet converged in this basis.

With CAP-EOM-EA-CCSD, such convergence problems does not arise because the CAP-HF equations are solved for the neutral molecule. Although it is not always trivial to identify the resonance state among the CAP-EOM-EA-CCSD solutions, we were able to identify the correct state of C_2H_4^- in basis sets with up to eight extra p -shells. The lower part of Tab. 5 illustrates that with six p -shells the position and width are converged to within 0.01 eV and 0.02 eV, respectively.

5 Conclusions

We have introduced a method for optimizing the onset of complex absorbing potentials that offer the possibility to compute energies and widths of molecular temporary anions in a basis set of atom-centered Gaussian functions. Our method is based on an error function that evaluates what fraction of the resonance position and width are due to the expectation value of the CAP. If the values of these fractions are close to one, the CAP exclusively acts as a perturbation and does not stabilize the resonance. Conversely, the closer the values are to zero, the less perturbed the resonance wave function is by the CAP. The new criterion can be viewed as a generalization of the established criterion for optimizing the CAP strength and can, in principle, be further generalized to arbitrary CAP parameters.

We tested our new approach for the π^* temporary anions of N_2 , C_2H_4 , and HCOOH using box CAPs and smooth Voronoi CAPs at the HF and EOM-EA-CCSD levels of theory. We also used the projected CAP-EOM-EA-CCSD method where the CAP is represented in a basis of CAP-free EOM-EA-CCSD states. The optimal onsets usually vary only little between box and smooth Voronoi CAP as well as between HF, full and projected EOM-EA-CCSD calculations. Overall, the performance of the new approach is similar to that of the established one in which the CAP strength is optimized although we found substantial discrepancies in the resonance width in some cases.

The computational cost of both approaches is ultimately comparable. Whereas the established technique entails the need to run series of calculations with different CAP strength, our new technique requires to run analogous series in which the onset parameters are varied. This equally applies to full and projected CAP calculations. Also, using a large enough CAP strength is important in the new approach just like choosing the onset properly is important in the established approach. Nonetheless, we believe that optimization of the CAP onset as proposed in the present work will prove useful to resolve pathological cases where optimization of only the CAP strength does not yield satisfactory results.

Acknowledgement

Funding from the European Research Council (ERC) under the European Union’s Horizon 2020 research and innovation program (Grant Agreement No. 851766) and the KU Leuven internal funds (Grant No. C14/22/083) is gratefully acknowledged. Resources and services used in this work were partly provided by the VSC (Flemish Supercomputer Center) funded by the Research Foundation—Flanders (FWO) and the Flemish Government.

References

- (1) Boudaïffa, B.; Cloutier, P.; Hunting, D.; Huels, M. A.; Sanche, L. Resonant Formation of DNA Strand Breaks by Low-Energy (3 to 20 eV) Electrons. *Science* **2000**, *287*, 1658–1660.
- (2) Simons, J. How Very Low-Energy (0.1–2 eV) Electrons Cause DNA Strand Breaks. *Adv. Quantum Chem.* **2007**, *52*, 171–188.
- (3) Millar, T. J.; Walsh, C.; Field, T. A. Negative Ions in Space. *Chem. Rev.* **2017**, *117*, 1765–1795.

- (4) Stoffels, E.; Stoffels, W. W.; Kroesen, G. M. W. Plasma chemistry and surface processes of negative ions. *Plasma Sources Sci. Technol.* **2001**, *10*, 311–317.
- (5) Herbert, J. M. The quantum chemistry of loosely-bound electrons. *Rev. Comp. Chem.* **2015**, *28*, 391–517.
- (6) Ingólfsson, O., Ed. *Low-Energy Electrons: Fundamentals and Applications*; Pan Stanford Publishing, 2019.
- (7) Moiseyev, N. *Non-Hermitian Quantum Mechanics*; Cambridge University Press, 2011.
- (8) Jagau, T.-C.; Bravaya, K. B.; Krylov, A. I. Extending Quantum Chemistry of Bound States to Electronic Resonances. *Annu. Rev. Phys. Chem.* **2017**, *68*, 525–553.
- (9) Jagau, T. C. Theory of electronic resonances: Fundamental aspects and recent advances. *Chem. Commun.* **2022**, *58*, 5205–5224.
- (10) Bardsley, J. N.; Mandl, F. Resonant scattering of electrons by molecules. *Rep. Prog. Phys.* **1968**, *31*, 471–531.
- (11) Taylor, J. R. *Scattering Theory: The Quantum Theory on Nonrelativistic Collisions*; Wiley, 1971.
- (12) Aguilar, J.; Combes, J. M. A class of analytic perturbations for one-body Schrödinger Hamiltonians. *Commun. Math. Phys.* **1971**, *22*, 269–279.
- (13) Balslev, E.; Combes, J. M. Spectral properties of many-body Schrödinger operators with dilatation-analytic interactions. *Commun. Math. Phys.* **1971**, *22*, 280–294.
- (14) Moiseyev, N. Quantum theory of resonances: calculating energies, widths and cross-sections by complex scaling. *Phys. Rep.* **1998**, *302*, 212–293.
- (15) McCurdy, C. W.; Rescigno, T. N. Extension of the Method of Complex Basis Functions to Molecular Resonances. *Phys. Rev. Lett.* **1978**, *41*, 1364–1368.

- (16) Moiseyev, N.; Corcoran, C. Autoionizing states of H_2 and H_2^- using the complex-scaling method. *Phys. Rev. A* **1979**, *20*, 814–817.
- (17) White, A. F.; Head-Gordon, M.; McCurdy, C. W. Complex basis functions revisited: Implementation with applications to carbon tetrafluoride and aromatic N-containing heterocycles within the static-exchange approximation. *J. Chem. Phys.* **2015**, *142*, 054103.
- (18) Jolicard, G.; Austin, E. J. Optical potential stabilization method for predicting resonance levels. *Chem. Phys. Lett.* **1985**, *121*, 106–110.
- (19) Jolicard, G.; Austin, E. J. Optical potential method of calculating resonance energies and widths. *Chem. Phys.* **1986**, *103*, 295–302.
- (20) Riss, U. V.; Meyer, H.-D. Calculation of resonance energies and widths using the complex absorbing potential method. *J. Phys. B: At. Mol. Opt. Phys.* **1993**, *26*, 4503–4535.
- (21) Muga, J. G.; Palao, J. P.; Navarro, B.; Egusquiza, I. L. Complex absorbing potentials. *Phys. Rep.* **2004**, *395*, 357–426.
- (22) Moiseyev, N.; Certain, P. R.; Weinhold, F. Resonance properties of complex-rotated Hamiltonians. *Mol. Phys.* **1978**, *36*, 1613–1630.
- (23) Siegert, A. J. F. On the Derivation of the Dispersion Formula for Nuclear Reactions. *Phys. Rev.* **1939**, *56*, 750–752.
- (24) Kosloff, R.; Kosloff, D. Absorbing boundaries for wave propagation problems. *J. Comput. Phys.* **1986**, *63*, 363–376.
- (25) Neuhauser, D.; Baer, M. The time-dependent Schrödinger equation: Application of absorbing boundary conditions. *J. Chem. Phys.* **1989**, *90*, 4351–4355.
- (26) Neuhauser, D.; Baer, M. The application of wave packets to reactive atom-diatom systems: A new approach. *J. Chem. Phys.* **1989**, *91*, 4651–4657.

- (27) Macías, D.; Brouard, S.; Muga, J. Optimization of absorbing potentials. *Chem. Phys. Lett.* **1994**, *228*, 672–677.
- (28) Riss, U. V.; Meyer, H.-D. Reflection-free complex absorbing potentials. *J. Phys. B: At. Mol. Opt. Phys.* **1995**, *28*, 1475–1493.
- (29) Riss, U. V.; Meyer, H.-D. Investigation on the reflection and transmission properties of complex absorbing potentials. *J. Chem. Phys.* **1996**, *105*, 1409–1419.
- (30) Riss, U. V.; Meyer, H.-D. The transformative complex absorbing potential method: a bridge between complex absorbing potentials and smooth exterior scaling. *J. Phys. B: At. Mol. Opt. Phys.* **1998**, *31*, 2279–2304.
- (31) Moiseyev, N. Derivations of universal exact complex absorption potentials by the generalized complex coordinate method. *J. Phys. B: At. Mol. Opt. Phys.* **1998**, *31*, 1431–1441.
- (32) Sommerfeld, T.; Ehara, M. Complex Absorbing Potentials with Voronoi Isosurfaces Wrapping Perfectly around Molecules. *J. Chem. Theory Comput.* **2015**, *11*, 4627–4633.
- (33) Gyamfi, J. A.; Jagau, T.-C. Ab Initio Molecular Dynamics of Temporary Anions Using Complex Absorbing Potentials. *J. Phys. Chem. Lett.* **2022**, *13*, 8477–8483.
- (34) Zhou, Y.; Ernzerhof, M. Calculating the Lifetimes of Metastable States with Complex Density Functional Theory. *J. Phys. Chem. Lett.* **2012**, *3*, 1916–1920.
- (35) Jagau, T.-C.; Zuev, D.; Bravaya, K. B.; Epifanovsky, E.; Krylov, A. I. A Fresh Look at Resonances and Complex Absorbing Potentials: Density Matrix-Based Approach. *J. Phys. Chem. Lett.* **2014**, *5*, 310–315.
- (36) Zuev, D.; Jagau, T.-C.; Bravaya, K. B.; Epifanovsky, E.; Shao, Y.; Sundstrom, E.; Head-Gordon, M.; Krylov, A. I. Complex absorbing potentials within EOM-CC family

- of methods: Theory, implementation, and benchmarks. *J. Chem. Phys.* **2014**, *141*, 024102.
- (37) Benda, Z.; Jagau, T.-C. Analytic gradients for the complex absorbing potential equation-of-motion coupled-cluster method. *J. Chem. Phys.* **2017**, *146*, 031101.
- (38) Sommerfeld, T.; Riss, U. V.; Meyer, H.-D.; Cederbaum, L. S.; Engels, B.; Suter, H. U. Temporary anions—calculation of energy and lifetime by absorbing potentials: the N_2^- $^2\Pi_g$ resonance. *J. Phys. B: At. Mol. Opt. Phys.* **1998**, *31*, 4107–4122.
- (39) Sommerfeld, T.; Santra, R. Efficient method to perform CAP/CI calculations for temporary anions. *Int. J. Quantum Chem.* **2001**, *82*, 218–226.
- (40) Feuerbacher, S.; Sommerfeld, T.; Santra, R.; Cederbaum, L. S. Complex absorbing potentials in the framework of electron propagator theory. II. Application to temporary anions. *J. Chem. Phys.* **2003**, *118*, 6188–6199.
- (41) Sajeev, Y.; Santra, R.; Pal, S. Analytically continued Fock space multireference coupled-cluster theory: Application to the $^2\Pi_g$ shape resonance in e- N_2 scattering. *J. Chem. Phys.* **2005**, *122*, 234320.
- (42) Pal, S.; Sajeev, Y.; Vaval, N. Analytically continued Fock space multi-reference coupled-cluster theory: Application to the shape resonance. *Chem. Phys.* **2006**, *329*, 283–289.
- (43) Ghosh, A.; Vaval, N.; Pal, S. Equation-of-motion coupled-cluster method for the study of shape resonance. *J. Chem. Phys.* **2012**, *136*, 234110.
- (44) Jagau, T.-C.; Krylov, A. I. Complex Absorbing Potential Equation-of-Motion Coupled-Cluster Method Yields Smooth and Internally Consistent Potential Energy Surfaces and Lifetimes for Molecular Resonances. *J. Phys. Chem. Lett.* **2014**, *5*, 3078–3085.
- (45) Kunitsa, A. A.; Granovsky, A. A.; Bravaya, K. B. CAP-XMCQDPT2 method for molecular electronic resonances. *J. Chem. Phys.* **2017**, *146*, 184107.

- (46) Benda, Z.; Rickmeyer, K.; Jagau, T.-C. Structure Optimization of Temporary Anions. *J. Chem. Theory Comput.* **2018**, *14*, 3468–3478.
- (47) Benda, Z.; Jagau, T.-C. Understanding Processes Following Resonant Electron Attachment: Minimum-Energy Crossing Points between Anionic and Neutral Potential Energy Surfaces. *J. Chem. Theory Comput.* **2018**, *14*, 4216–4223.
- (48) Thodika, M.; Fennimore, M.; Karsili, T. N. V.; Matsika, S. Comparative study of methodologies for calculating metastable states of small to medium-sized molecules. *J. Chem. Phys.* **2019**, *151*, 244104.
- (49) Phung, Q. M.; Komori, Y.; Yanai, T.; Sommerfeld, T.; Ehara, M. Combination of a Voronoi-Type Complex Absorbing Potential with the XMS-CASPT2 Method and Pilot Applications. *J. Chem. Theory Comput.* **2020**, *16*, 2606–2616.
- (50) Gayvert, J. R.; Bravaya, K. B. Application of Box and Voronoi CAPs for Metastable Electronic States in Molecular Clusters. *J. Phys. Chem. A* **2022**, *126*, 5070–5078.
- (51) Gayvert, J. R.; Bravaya, K. B. Projected CAP-EOM-CCSD method for electronic resonances. *J. Chem. Phys.* **2022**, *156*, 094108.
- (52) Dempwolff, A. L.; Belogolova, A. M.; Sommerfeld, T.; Trofimov, A. B.; Dreuw, A. CAP/EA-ADC method for metastable anions: Computational aspects and application to π^* resonances of norbornadiene and 1,4-cyclohexadiene. *J. Chem. Phys.* **2021**, *155*, 054103.
- (53) Stanton, J. F.; Bartlett, R. J. The equation of motion coupled-cluster method. A systematic biorthogonal approach to molecular excitation energies, transition probabilities, and excited state properties. *J. Chem. Phys.* **1993**, *98*, 7029–7039.
- (54) Nooijen, M.; Bartlett, R. J. Equation of motion coupled cluster method for electron attachment. *J. Chem. Phys.* **1996**, *102*, 3629–3647.

(55) Epifanovsky, E.; Gilbert, A. T. B.; Feng, X.; Lee, J.; Mao, Y.; Mardirossian, N.; Pokhilko, P.; White, A. F.; Coons, M. P.; Dempwolff, A. L.; Gan, Z.; Hait, D.; Horn, P. R.; Jacobson, L. D.; Kaliman, I.; Kussmann, J.; Lange, A. W.; Lao, K. U.; Levine, D. S.; Liu, J.; McKenzie, S. C.; Morrison, A. F.; Nanda, K. D.; Plasser, F.; Rehn, D. R.; Vidal, M. L.; You, Z.-Q.; Zhu, Y.; Alam, B.; Albrecht, B. J.; Al-dossary, A.; Alguire, E.; Andersen, J. H.; Athavale, V.; Barton, D.; Begam, K.; Behn, A.; Bellonzi, N.; Bernard, Y. A.; Berquist, E. J.; Burton, H. G. A.; Carreras, A.; Carter-Fenk, K.; Chakraborty, R.; Chien, A. D.; Closser, K. D.; Cofer-Shabica, V.; Dasgupta, S.; de Wergifosse, M.; Deng, J.; Diedenhofen, M.; Do, H.; Ehlert, S.; Fang, P.-T.; Fatehi, S.; Feng, Q.; Friedhoff, T.; Gayvert, J.; Ge, Q.; Gidofalvi, G.; Goldey, M.; Gomes, J.; González-Espinoza, C. E.; Gulania, S.; Gunina, A. O.; Hanson-Heine, M. W. D.; Harbach, P. H. P.; Hauser, A.; Herbst, M. F.; Hernández Vera, M.; Hodecker, M.; Holden, Z. C.; Houck, S.; Huang, X.; Hui, K.; Huynh, B. C.; Ivanov, M.; Jász, A.; Ji, H.; Jiang, H.; Kaduk, B.; Kähler, S.; Khistyayev, K.; Kim, J.; Kis, G.; Klunzinger, P.; Koczor-Benda, Z.; Koh, J. H.; Kosenkov, D.; Koulias, L.; Kowalczyk, T.; Krauter, C. M.; Kue, K.; Kunitsa, A.; Kus, T.; Ladjánszki, I.; Landau, A.; Lawler, K. V.; Lefrancois, D.; Lehtola, S.; Li, R. R.; Li, Y.-P.; Liang, J.; Liebenthal, M.; Lin, H.-H.; Lin, Y.-S.; Liu, F.; Liu, K.-Y.; Loipersberger, M.; Luenser, A.; Manjanath, A.; Manohar, P.; Mansoor, E.; Manzer, S. F.; Mao, S.-P.; Marenich, A. V.; Markovich, T.; Mason, S.; Maurer, S. A.; McLaughlin, P. F.; Menger, M. F. S. J.; Mewes, J.-M.; Mewes, S. A.; Morgante, P.; Mullinax, J. W.; Oosterbaan, K. J.; Paran, G.; Paul, A. C.; Paul, S. K.; Pavošević, F.; Pei, Z.; Prager, S.; Proynov, E. I.; Rák, a.; Ramos-Cordoba, E.; Rana, B.; Rask, A. E.; Rettig, A.; Richard, R. M.; Rob, F.; Rossomme, E.; Scheele, T.; Scheurer, M.; Schneider, M.; Sergueev, N.; Sharada, S. M.; Skomorowski, W.; Small, D. W.; Stein, C. J.; Su, Y.-C.; Sundstrom, E. J.; Tao, Z.; Thirman, J.; Tornai, G. J.; Tsuchimochi, T.; Tubman, N. M.; Veccham, S. P.; Vydrov, O.; Wenzel, J.; Witte, J.; Yamada, A.; Yao, K.; Yeganeh, S.; Yost, S. R.;

- Zech, A.; Zhang, I. Y.; Zhang, X.; Zhang, Y.; Zuev, D.; Aspuru-Guzik, A.; Bell, A. T.; Besley, N. A.; Bravaya, K. B.; Brooks, B. R.; Casanova, D.; Chai, J.-D.; Coriani, S.; Cramer, C. J.; Cserey, G.; DePrince, A. E.; DiStasio, R. A.; Dreuw, A.; Dunietz, B. D.; Furlani, T. R.; Goddard, W. A.; Hammes-Schiffer, S.; Head-Gordon, T.; Hehre, W. J.; Hsu, C.-P.; Jagau, T.-C.; Jung, Y.; Klamt, A.; Kong, J.; Lambrecht, D. S.; Liang, W.; Mayhall, N. J.; McCurdy, C. W.; Neaton, J. B.; Ochsenfeld, C.; Parkhill, J. A.; Peverati, R.; Rassolov, V. A.; Shao, Y.; Slipchenko, L. V.; Stauch, T.; Steele, R. P.; Subotnik, J. E.; Thom, A. J. W.; Tkatchenko, A.; Truhlar, D. G.; Van Voorhis, T.; Wesolowski, T. A.; Whaley, K. B.; Woodcock, H. L.; Zimmerman, P. M.; Faraji, S.; Gill, P. M. W.; Head-Gordon, M.; Herbert, J. M.; Krylov, A. I. Software for the frontiers of quantum chemistry: An overview of developments in the Q-Chem 5 package. *J. Chem. Phys.* **2021**, *155*, 084801.
- (56) Gilbert, A. T. B.; Besley, N. A.; Gill, P. M. W. Self-Consistent Field Calculations of Excited States Using the Maximum Overlap Method (MOM). *J. Phys. Chem. A* **2008**, *112*, 13164–13171.
- (57) Becke, A. D. A multicenter numerical integration scheme for polyatomic molecules. *J. Chem. Phys.* **1988**, *88*, 2547–2553.
- (58) Berman, M.; Estrada, H.; Cederbaum, L. S.; Domcke, W. Nuclear dynamics in resonant electron-molecule scattering beyond the local approximation: The 2.3-eV shape resonance in N₂. *Phys. Rev. A* **1983**, *28*, 1363–1381.
- (59) Jagau, T.-C.; Krylov, A. I. Characterizing metastable states beyond energies and lifetimes: Dyson orbitals and transition dipole moments. *J. Chem. Phys.* **2016**, *144*, 054113.
- (60) Walker, I. C.; Stamatovic, A.; Wong, S. F. Vibrational excitation of ethylene by electron impact: 1–11 eV. *J. Chem. Phys.* **1978**, *69*, 5532–5537.

- (61) Panajotovic, R.; Kitajima, M.; Tanaka, H.; Jelisavcic, M.; Lower, J.; Campbell, L.; Brunger, M. J.; Buckman, S. J. Electron collisions with ethylene. *J. Phys. B: At. Mol. Opt. Phys.* **2003**, *36*, 1615–1626.
- (62) White, A. F.; Epifanovsky, E.; McCurdy, C. W.; Head-Gordon, M. Second order Møller-Plesset and coupled cluster singles and doubles methods with complex basis functions for resonances in electron-molecule scattering. *J. Chem. Phys.* **2017**, *146*, 234107.
- (63) Aflatooni, K.; Hitt, B.; Gallup, G. A.; Burrow, P. D. Temporary anion states of selected amino acids. *J. Chem. Phys.* **2001**, *115*, 6489–6494.
- (64) Hocking, W. H. The Other Rotamer of Formic Acid, cis-HCOOH. *Z. Naturforsch. A* **1976**, *31*, 1113–1121.
- (65) Rescigno, T. N.; Trevisan, C. S.; Orel, A. E. Dynamics of Low-Energy Electron Attachment to Formic Acid. *Phys. Rev. Lett.* **2006**, *96*, 213201.
- (66) Pelc, A.; Sailer, W.; Scheier, P.; Probst, M.; Mason, N. J.; Illenberger, E.; Märk, T. D. Dissociative electron attachment to formic acid (HCOOH). *Chem. Phys. Lett.* **2002**, *361*, 277–284.
- (67) Allan, M. Study of resonances in formic acid by means of vibrational excitation by slow electrons. *J. Phys. B: At. Mol. Opt. Phys.* **2006**, *39*, 2939–2947.
- (68) Vizcaino, V.; Jelisavcic, M.; Sullivan, J. P.; Buckman, S. J. Elastic electron scattering from formic acid (HCOOH): absolute differential cross-sections. *New J. Phys.* **2006**, *8*, 85.
- (69) Dunning, T. H. Gaussian basis sets for use in correlated molecular calculations. I. The atoms boron through neon and hydrogen. *J. Chem. Phys.* **1989**, *90*, 1007–1023.
- (70) Kendall, R. A.; Dunning, T. H.; Harrison, R. J. Electron affinities of the first-row

atoms revisited. Systematic basis sets and wave functions. *J. Chem. Phys.* **1992**, *96*, 6796–6806.